Proceedings of ASME Turbo Expo 2011
GT2011
June 6-10, 2011, Vancouver, Canada

GT2011-45953

A REVISED EQUATION FOR HEAT FLUX REDUCTION IN FILM COOLING STUDIES AND DISCUSSION OF ITS APPLICATIONS

Ting Wang and Lei Zhao
Energy Conversion and Conservation Center
University of New Orleans
New Orleans, LA 70148-2220, USA
Emails: lzhao@uno.edu; twang@uno.edu

ABSTRACT

In film cooling experimental studies, due to the difficulty in measuring the surface heat flux variation, a Heat Flux Ratio (HFR) equation originally derived by Mick and Mayle [1], has been widely employed to calculate the surface heat flux distribution using the measured adiabatic film effectiveness and surface temperature. A close examination of the derivation process and applications of the HFR equation reveals two issues of concern. First, an implicit assumption was introduced by letting the wall surface temperature of the system without-film be the same as that which would occur with a film-cooled condition. A revised equation is then derived by removing this implicit assumption and incorporating the wall temperature change due to film cooling Secondly, a uniform value of the non-dimensional metal temperature φ (or film cooling effectiveness) has been used in all the previous applications of the HFR equation. This practice implicitly implies that a uniform wall temperature is distributed throughout the entire surface under film cooling, which is usually not the case in real conditions.

A series of computational experiments are conducted to verify the revised HFR equation under different conditions as well as examine the validity of using a constant surface temperature in the HFR equation. Results reveal that using a constant value of φ (0.5 ~ 0.7) to calculate surface heat flux may result in a negative HFR in some simulated cases showing the commonly adopted value φ=0.5~0.7. This could induce errors and give false HFR. The error is reduced in 3D cases because the streamwise wall temperature becomes more uniform than 2D cases. The difference between the old and new equations can reach about 20%. A conjugate wall cooling simulation shows negative HFR is possible in the region close to the film hole due to the heat conduction from the downstream hotter region into the cooler region near the film hole. Using the actual wall temperature as the φ-value, the newly revised HFR equation produces the exact heat flux as calculated by CFD including the correct calculation of negative heat flux caused by the conjugate wall.

NOMENCLATURE

b	coolant injection slot width (mm)
h_{af}	adiabatic film heat transfer coefficient ($h_{af} = q'' / (T_{aw}-T_w)$) ($W/m^2K$)
HFR	heat flux ratio (q'' / q''_o)
k	turbulence kinetic energy (m^2/s^2)
l	chord length (mm)
M	blowing ratio, $(\rho u)_j/(\rho u)_g$
Nu_x	Nusselt number, hx/λ, x is the distance from the injection hole in streamwise direction
NHFR	net heat flux reduction ($1- q'' / q''_o$)
Pr	Prandtl number (ν/α)
q"	heat flux (W/m^2), positive value for heat flowing from gas into the wall
r	recovery factor
Re_l	Reynolds number based on chord length, ul/ν
T_{aw}	adiabatic wall temperature (K)
T_w	wall surface temperature in contact with gas (K)
T_g	main gas flow temperature (K)
T_j	coolant temperature at the cooling jet hole exit (K)
T_{ci}	internal coolant temperature (K)
T_r	recovery temperature (K)
T_u	turbulence intensity

Greek Letters

α	thermal diffusivity (m^2/s)
ε	turbulence dissipation rate (m^2/s^3)
η	adiabatic film cooling effectiveness, $(T_g-T_{aw})/(T_g-T_j)$
λ	heat conductivity (W/mK)
ν	kinematic viscosity (m^2/s)
$\rho\overline{u'v'}$	Reynolds stress
φ	film cooling effectiveness, $\varphi = (T_g-T_w) / (T_g-T_j)$ (or non-dimensional metal temperature, overall cooling effectiveness)

Subscripts

aw	adiabatic wall
ci	internal cooling
conj	conjugate blade
f	with film cooling
g	main flow of hot gas/air
j	coolant or jet flow
o	without film
w	wall

INTRODUCTION

Film cooling has been widely used in high-performance gas turbines to protect turbine airfoils from being damaged by hot flue gases. Film injection holes are placed in the body of the airfoil to allow coolant to pass from the internal cavity to the external surface. The ejection of coolant gas results in a layer or "film" of coolant gas flowing along the external surface of the airfoil. Hence, the term "film cooling" is used to describe this cooling scheme.

The ultimate goal of introducing film cooling to turbine airfoils is to reduce the heat load on the blade, i.e. reduce surface heat flux and/or lowers the airfoil's temperature, so the life of turbine airfoils can be significantly extended. Thus it is always desired to know how much heat flux or blade temperature can be actually reduced after film cooling is employed. However, due to the experimental difficulty in directly measuring the heat flux, the **Heat Flux Ratio (HFR)** $q" / q"_o$ is often evaluated indirectly through a theoretical relation developed by Mick and Mayle [1] between two characteristic factors of film cooling heat transfer: adiabatic film effectiveness (η) and film heat transfer coefficients (h_{af} and h_o), as:

$$q" / q"_o = (h_{af} / h_o)\,(1-\eta/\varphi) \quad (1)$$

In which, the **adiabatic film effectiveness** is defined as:

$$\eta = (T_g-T_{aw}) / (T_g-T_j) \quad (2)$$

Where T_g is the main flow hot gas temperature, T_j is the coolant temperature at the cooling jet hole exit, and T_{aw} is the adiabatic wall temperature. η is an excellent indicator of film cooling performance by comparing the insulated wall surface temperature (T_{aw}) with the would-be perfect cooled wall temperature, T_j. If the film cooling were perfect, η =1 and the wall is protected as cold as the cooling jet temperature. The **adiabatic film heat transfer coefficient** is defined as:

$$h_{af} = q" / (T_{aw}-T_w) \quad (3)$$

where T_w is the airfoil wall surface temperature that comes immediately in contact with the hot main gas flow. This definition is clear if the wall boundary condition is not adiabatic, which means that the actual wall heat flux would be driven by the potential adiabatic wall temperature T_{aw}.

In Eq. 1, the local heat flux without film cooling is given as:

$$q"_o = h_o\,(T_g-T_w) \quad (4)$$

the **film cooling effectiveness**, φ, is defined as:

$$\varphi = (T_g-T_w) / (T_g-T_j) \quad (5)$$

The definition of φ is very similar to η except T_{aw} in Eq. 2 is replaced with T_w. To reduce complexity, T_j is assumed the same as the internal coolant temperature, T_{cj}. Although we can say that η is a special case of the more generically defined film cooling effectiveness (φ) when the wall is insulated, it is convenient to use both terms by designating φ for all non-adiabatic wall conditions and η only for the adiabatic wall condition. φ has also been called **non-dimensional metal temperature** (The Gas Turbine Handbook [2]) or the **overall cooling effectiveness** in other literatures. The term "film cooling effectiveness" is preferred in this paper because the other two terms do not specifically indicate the physics of applying the cooling "film."

For a perfect film cooling performance, the film cooling effectiveness would have a value of unity (η or φ = 1.0), i.e. T_{aw} is equal to the coolant temperature (T_j) at the exit of the jet injection hole; while a value of η or φ = 0 means that the film cooling has no effect in reducing the wall temperature, which is maintained as hot as the mainstream gas.

Clarification of terminology is needed for HFR, since in some literatures it is referred to as the Heat Flux Reduction which originated from the study of Mick and Mayle [1]. But from the definition, it is actually the ratio of heat fluxes with film over that without film. Thus $q" / q"_o$ in Eq. 1 is more appropriately called Heat Flux Ratio, rather than Heat Flux Reduction. Meanwhile, Net Heat Flux Reduction (NHFR) was introduced by Bogard's group at the University of Texas as $NHFR=1- q" / q"_o=1- (h_{af} / h_o)\,(1-\eta/\varphi)$, which describes the ratio of reduced heat flux amount with film cooling over the heat flux without film cooling. In this study, HFR is referred to as the Heat Flux Ratio and this term will be employed throughout this paper.

In a real gas turbine, the airfoils are cooled inside by internal coolant flow and part of the coolant is bled and utilized for external film cooling. Therefore, the actual heat transfer path goes through a conjugate condition from hot main flow gas to the airfoil surface via convection and radiation, spreads over the airfoil material via conduction, and then transfers to the internal cooling fluid via convection again. The ultimate energy source is the hot gases in the main flow and the energy sinks are the internal flow and film flow. Due to the complexity of this conjugate heat transfer condition, many film cooling experiments have been performed under simplified conditions such as applying an adiabatic wall condition or uniformly heated wall condition. Therefore, it is always highly desired to know HFR through Eq. 1.

Eq.1 is mathematically derived, so it is theoretically correct. In order to determine the value of $q"/q_o"$ through experiments, two tests need to be performed: one for the adiabatic case to acquire η and the other for the conjugate case (with and without film) for h_{af} / h_o. But how can φ be obtained? Based on the derivation by the original producers of this equation, Mick and Mayle [1], φ is claimed to be typically about 0.6 for modern gas turbine components; however, no supporting material or data were provided in their paper to substantiate this value. This value of "0.6" has been widely used and cited since 1988, for example in [3] and [4]. Examination of the φ definition in Eq. 5 unequivocally indicates that the value "0.6" implies the film cooling effectiveness is 0.6 under non-adiabatic conditions. It is understood that HFR calculated using a pre-assumed φ value could serve as an estimate for film cooling scheme applied in an assumed condition, but this practice brings about several issues of concern. The first issue is that this single constant value can hardly be valid for various cases of different conditions irrespective of the influence from parameters such as jet temperature, blowing ratio, hole configurations, etc. The second issue is that film cooling effectiveness should actually

be non-uniform along the surface, thus applying a constant φ-value everywhere is questionable. The third issue is that a constant φ-value implies a constant wall surface temperature, which does not represent real film cooling conditions. The fourth issue is that since the value of 0.6 was assumed for real gas turbine environment, it is questionable that this same value is appropriate for use in low temperature laboratory conditions. Oh and Han [4] and Lu et al. [5] expanded the range of φ value from 0.6 to between 0.5 and 0.7, but no supporting material was found either for what φ value should be used under what conditions. Therefore, the practices of assigning or assuming a single value of φ are questionable and not convincing.

Furthermore, if Eq.1 is used to calculate q", h_{af} will need to be calculated from Eq.3 by measuring T_w distribution from an experiment. If T_w-values are measured from the experiment, φ-values can be directly calculated through Eq.5 and then used in calculating HFR in Eq.1. Instead, many researchers employed an assumed single φ-value (0.6 or any other values) for calculating HFR despite the available φ-values in their specific study.

A sketch is shown in Fig. 1 to qualitatively illustrate the heat transfer scenario including the temperature profiles at two locations: one near the jet injection hole with a possible reversed heat flow and the other located further downstream from the injection hole region. The slopes of the temperature profiles are drawn to qualitatively reflect the heat flow directions.

The objective of this paper is to systematically investigate the above issues guided by CFD simulations.

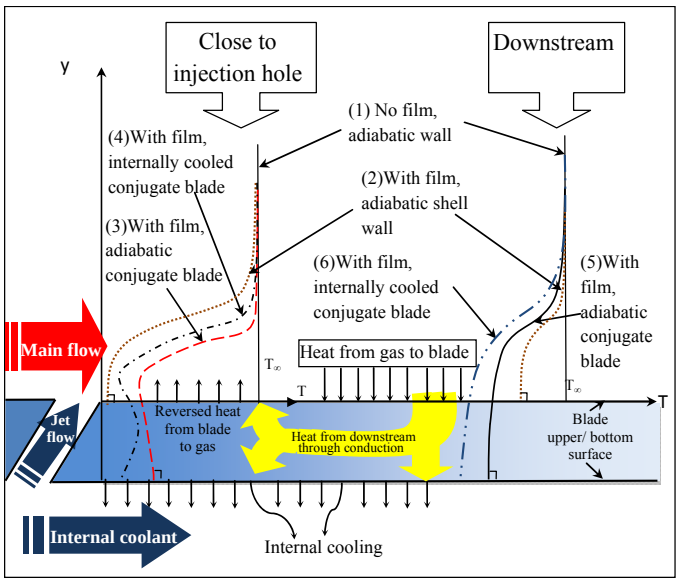

Figure 1 Qualitative temperature profiles of a typical internally and film cooled airfoil at two locations: one near the injection hole region with potentially reversed heat transfer and the other located further downstream. (Note, the internal coolant flow can direct into and out of the paper alternately in some applications.)

MODELING AND METHODOLOGY

The investigation in this paper is guided by a series of computational fluid dynamic (CFD) simulations. Although the actual numerical values of CFD are often subject to uncertainties from different turbulence models, discretization resolution, and grid quality, the global heat transfer and flow physics can be captured relatively trustfully in modern CFD schemes. Since the focus of this study is on the thermal-flow physics and relative comparisons of different cases, any bias generated by the CFD scheme is generally not so critical in the comparative nature of the analysis conducted in this paper.

Considering that experimental film cooling studies using low temperature and low heat flux laboratory conditions have been more commonly seen in open literatures than those employing real engine conditions, in this study, the issues will be discussed based on simulations of lab conditions first and followed by imposing elevated conditions in real gas turbines.

Geometrical Configuration

To make analysis easier, 2D conditions with various changing parameters are simulated first; 3D cases will follow to add the impacts from the complexity of the 3D flow structure. In the 2D cases, a slot is selected; its configuration and the main dimensions are shown in Fig. 2. A 3D study is then built upon the geometry set-up of the 2D studies, with a pitch to diameter ratio (p/b) of 3.

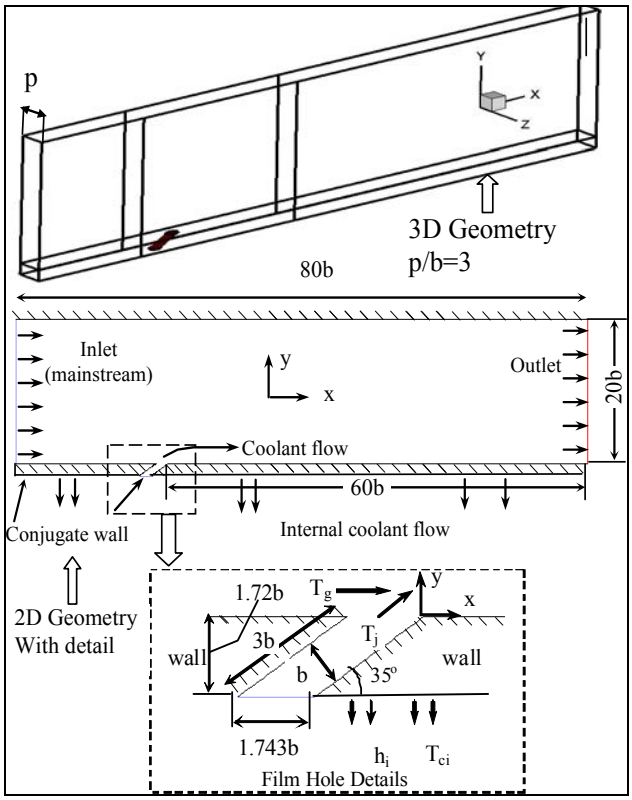

Figure 2 Computational domains for 2D and 3D respectively

The slot width (b) is 4 mm. The injection angle is 35°, which is considered as the optimal value by Bell et al. [6] and Brittingham et al. [7]. The length of the film slot is 3b from the coolant supply plenum to the surface. The computational domain has a length of 80b and a height of 20b. The slot jet is set to 20b from the entrance of the mainstream. In the conjugate cases arrangement, the solid metal wall with a

uniform thickness of 1.72b is included in the computational domain. An internal cooling channel flow is imposed below the base wall bottom surface, with an internal heat transfer coefficient h_i and a coolant flow temperature T_{ci} as shown in Fig. 2. It is understood that plenum and film injection hole conditions have important effects on film cooling performance and there are numerous research papers focusing on those topics, but since this paper is not aimed for studying film cooling performance, and also for the purpose of simplifying the analysis and focusing on the HFR issues, a plenum is not included and the adiabatic wall condition is assumed within the film injection wall.

Governing Equations

The time-averaged, steady-state Navier-Stokes equations as well as equations for mass, energy and species transport are solved. The governing equations for conservation of mass, momentum, and energy are given as:

$$\frac{\partial}{\partial x_i}(\rho u_i) = S_m \tag{6}$$

$$\frac{\partial}{\partial x_i}(\rho u_i u_j) = \rho \bar{g}_j - \frac{\partial P}{\partial x_j} + \frac{\partial}{\partial x_i}\left(\tau_{ij} - \rho\overline{u'_i u'_j}\right) + F_j \tag{7}$$

$$\frac{\partial}{\partial x_i}(\rho c_p u_i T) = \frac{\partial}{\partial x_i}\left(\lambda \frac{\partial T}{\partial x_i} - \rho c_p \overline{u'_i T'}\right) + \mu\Phi + S_h \tag{8}$$

where τ_{ij} is the symmetric stress tensor defined as

$$\tau_{ij} = \mu\left(\frac{\partial u_j}{\partial x_i} + \frac{\partial u_i}{\partial x_j} - \frac{2}{3}\delta_{ij}\frac{\partial u_k}{\partial x_k}\right). \tag{9}$$

$\mu\Phi$ is the viscous dissipation and λ is the heat conductivity.

Notice the terms of $\rho\,\overline{u'_i u'_j}$, and $c_p\,\overline{u'_i T'}$ represent the Reynolds stresses and turbulent heat fluxes, which should be modeled properly for a turbulent flow. The Reynolds number of the main flow (based on the duct height and the inlet condition specified later) is about 50,000 in this study.

Boundary Conditions

All walls have a non-slip velocity boundary condition in this study. Flow conditions with low temperature, pressure, and velocity for typical laboratory experiments are employed. For conjugate cases, Inconel X-750 properties are used for blade material with variable properties as functions of temperature. A heat transfer coefficient of h_i = 100 W/m^2-K and coolant flow temperature T_{ci} = 300K are assigned to the internal cooling flow, which is located at the bottom of Fig. 2. Air is modeled as an incompressible ideal gas with the density varying with temperature and the heat capacity modeled as a piecewise polynomial function of temperature with two temperature sub-ranges of 100-1000K and 1000-2000K, respectively. Inlet and outlet conditions, wall thermal boundary conditions for cases under lab conditions are summarized in Table 1. Details of the cases set-up will be shown later in this section.

Numerical Method

The commercial software code Fluent (version 6.2.16) from Ansys, Inc. is adopted in this study. The simulation uses the segregated solver, which employs an implicit pressure-correction scheme [8]. The SIMPLE algorithm is used to couple the pressure and velocity. The second order upwind scheme is selected for spatial discretization of the convective terms.

As shown in Fig. 3, structured but non-uniform grids are constructed for 2D studies. The grids near the jet wall and the wall surface are denser than the other areas. A grid independence study is conducted by comparing adiabatic film effectiveness of simulations based on two different meshes of 80,000 and 48,000 cells respectively. The results are almost identical. The mesh adopted in this study is of 400 grids in the x-direction and 120 in the y-direction for 2D studies. Unstructured grids are employed for the 3D studies with finer grids near the injection hole and the top surface. Less than 5% difference in adiabatic film effectiveness on centerline is found from the simulations based on meshes of 1.24 million cells versus772,000 cells. Due to the limit of the existing RAM limit in the personal computers, the grid of 1.24 million cells is used in this study.

Converged results are obtained after the specified residuals are met. A converged result renders a mass residual of 10^{-5}, energy residual of 10^{-7}, and momentum and turbulence kinetic energy residuals of 10^{-6}. These residuals are the summation of the imbalance for each cell, scaled by a representative of the flow rate. Typically, 1000 to 2000 iterations are needed to obtain a converged result, which takes about 2 hours on a parallel computer cluster consisting of eight nodes of 2.53 GHz Pentium dual-core personal computers.

Table. 1. Summary of Boundary Conditions

		2-D hole	
Operational pressure	P (atm)	1	
Main stream inlet	T_g (K)	400	400K=260.6°F
	u_g (m/s)	10	Uniform
	Tu (%)	3	Turbulence Intensity
	$Re_l \times 10^{-6}$	0.21	l=0.32m
Jet inlet	T_j (K)	300	300 K = 80.6°F
	u_j (m/s)	10	Uniform
	Tu (%)	3	Turbulence intensity
	$Re_d \times 10^{-3}$	2.67	d=4mm
$M=(\rho u)_j/(\rho u)_g$	M	1.3	blowing rato
Outlet	P (atm)	1	Constant pressure
Conjugate cooling wall	T_{ci} (K)	300	
	h_i (W/m^2-K)	100	

CFD Model Qualification and Uncertainty Estimate

The effect of turbulence models on cooling effectiveness using the same 2D mesh has been investigated in a previous study by Li and Wang [9] and is not repeated here. The 3D CFD benchmark case using five different turbulence models is carried out. The simulation results of spanwise-averaged adiabatic film cooling effectiveness for the case M = 0.5 are compared with the experimental data of Goldstein et al. [10]. The results of five turbulence models are plotted in Fig 4. The standard k-ε model with enhanced near-wall treatment gives the best agreement with the experimental data and is hereby employed in this study. The Y^+ values of the first near-wall cell from the qualification case are below 0.8 for most X locations (Fig. 5).

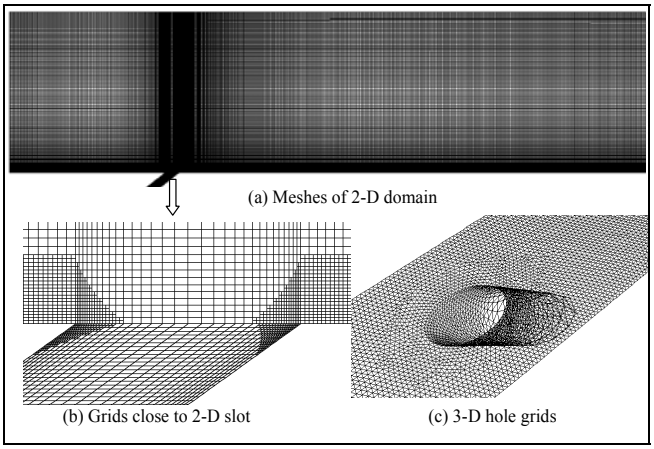

Figure 3 Computational Meshes for 2D and 3D domains respectively

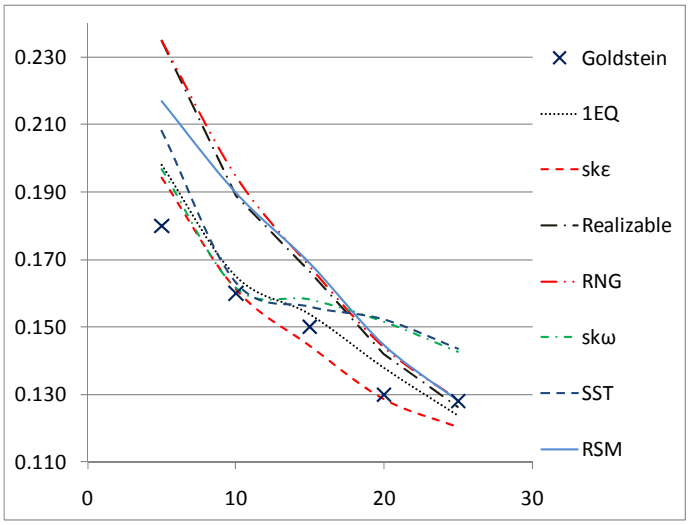

Figure 4 Comparison of CFD result with the experiment result of Goldstein [10]

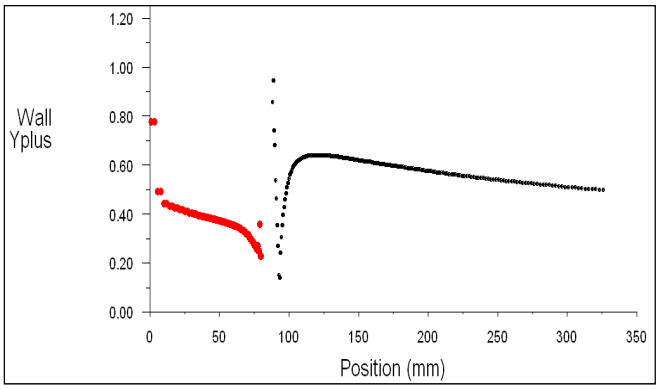

Figure 5 Y^+ distribution of the first mesh near the wall

The uncertainty from the key factors are estimated as: 10% for 3 different turbulence models, 5% for turbulence length scales, 3% for resolution of second order central and upwind methods, 1% for convergence resolution, 5% for the effect of grid size, and 3% for the near-wall grid effect. The overall uncertainty for cooling effectiveness is estimated to be 13% using the root-mean-square method. The above uncertainty is estimated from the computational results under low temperature and pressure conditions. Therefore, the estimated uncertainty is not centered with the true value; rather it represents the uncertainty excursion of the results that are attributed by the computational model and scheme.

Methodology and Cases Set-up

The conjugate heat transfer scenario of an operational turbine airfoil film cooling system consists of a main flow of hot gas with known conditions riding along the airfoil's upper surface, with the internal coolant flow moving underneath the airfoil's bottom surface and a portion of the coolant being injected through the coolant holes over the airfoil surface. The airfoil wall temperature and heat flux are determined by those conditions. The most appropriate simulation of this film-cooling system is to set up the main flow, internal flow and film injection conditions as boundary conditions while leaving the airfoil's wall thickness as part of the conjugate calculation. Also to evaluate the heat flux reduction on the airfoil, the heat transfer of the same system running without film injection needs to be simulated. The simulated cases are described below.

Case 1 Without-film, internally cooled conjugate case in 2D

Case 2 With-film, internally cooled conjugate case in 2D (**Baseline Case**)

The HFR calculated completely based on the simulation results of the two cases is referred to as the CFD HFR of a system, as opposed to the HFR obtained from Eq. 1 with the additional information of h_{af}, h_o, and η.

To evaluate Eq. 1 for HFR calculation, a simulation of the adiabatic case is needed to acquire η. Considering the conjugate airfoil condition, two approaches can be taken to simulate the adiabatic boundary condition: (1) adiabatic wall condition is imposed on the upper wall surface and the airfoil's wall is not included in the calculation (**shell wall** approach) (2) The adiabatic condition is applied to the inner (or bottom) surface of the airfoil and the airfoil's wall is included in the calculation (**finite wall** approach). The comparison of the two cases has been extensively discussed in the study of Zhao and Wang [11], which concluded that the adiabatic temperature obtained from the shell wall condition is more accurate to indicate the correct heat flux direction when the internal cooling is applied. Therefore, the shell wall condition is applied in this study.

Case 3 Film-cooled adiabatic wall case in 2D

With the results of Cases 1, 2 and 3, all the parameters needed to calculate HFR using Eq. 1 can be readily acquired through Case 1 (h_o), Case 2 (h_{af}), and Case 3 (η). Three values for φ, 0.4 0.6 and 0.9 are adopted for calculation of HFR; among which the values of φ=0.4 and 0.6 are popular values used in many film cooling literatures. In addition, T_w obtained from Case 2 via CFD is also employed to calculate the corresponding HFR using Eq. 1. The HFR values calculated from Eq. 1 are then compared with the HFR value completely obtained from the CFD simulations.

Even though the cases studied at this point are simulated under a typical laboratory condition, the discussions and conclusions are not expected to be significantly affected by the different operating conditions in an elevated gas turbine condition. The underlying fundamental physics and methodology are the same regardless of the operating condition because the discussions are also based on normalized value of φ and η and are focused on methodology of the practices. To support this statement, cases under elevated conditions are simulated accordingly. The simulated GT operating condition represents a general condition in an F-frame type GT without trying to match the specific condition of any brand name or model. The material properties and boundary conditions in a typical F-frame GT are summarized in Table 2. Variable properties of both air and blade are adopted as a function of temperature and pressure.

Table. 2. Summary of conditions and material properties under a typical F-type real engine condition

Engine condition			
Operational pressure	P (atm)	15	
Main stream inlet	T_g (K)	1400	2060°F
	u_g(m/s)	80	Uniform
	Tu	3%	Turbulence Intensity
	$Re_l x10^{-6}$	1.6	l=0.32m
Jet inlet	T_j(K)	750	890°F
	u_j (m/s)	56	Mach=0.1, Uniform
	Tu	3%	Turbulence intensity
	$Re_d x10^{-6}$	0.05	d=4mm
$M=(\rho u)_j/(\rho u)_g$	M	1.3	Blowing ratio
Outlet	P (atm)	15	Constant pressure
Conjugate cooling wall	T_{ci} (K)	750	
	h_i (W/m^2-K)**	1800	
Blade*	k (W/m-K)	16.9	at T=422K
		26.5	at T=811K
		31.4	at T=1033K
		35.3	at T=1144K
Air	ρ (kg/m^3)	3.43	at T=1400K, P=15 atm
	k (W/m-K)	0.1	
	μ (x10^{-6} kg/m-s)	55.7	
	ν (x10^{-6} m^2/s)	16	

Case 4 Simulations at Elevated Gas Turbine Operating Condition

Case 4.1 Without-film, internally cooled conjugate case
Case 4.2 With-film, internally cooled conjugate case
Case 4.3 Film-cooled adiabatic shell wall case

The 3Dcases are designed following the corresponding condition in each of the 2D cases. All simulated cases are summarized in Table 3 and illustrated in Fig. 6.

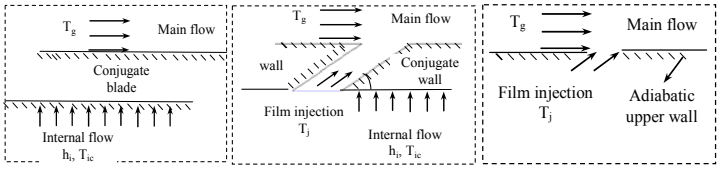

Case 1 Case 4.1 Case 5 Case 2 Case 4.2 Case 6 Case 3 Case 4.3 Case 7

Figure 6 Illustrations of boundary condition set-up for different cases

Case 5 Without-film, internally cooled conjugate case in 3D
Case 6 With-film, internally cooled conjugate case in 3D
Case 7 Film-cooled, adiabatic wall case in 3D

Table 3 Summary of Cases Set-up

Case #	Film Existence	Thermal Boundary Condition	Dimen
Case 1	without film	internal cooling, conjugate, lab condition	2D
Case 2	with film	internal cooling, conjugate, lab condition	2D
Case 3	with film	adibatic, lab condition	2D
Case 4.1	without film	internal cooling, conjuate, elevated gas turbine condition	2D
Case 4.2	with film	internal cooling, conjuate, elevated gas turbine condition	2D
Case 4.3	with film	adiabatic, elevated gas turbine condition	2D
Case 5	without film	internal cooling, conjugate, lab condition	3D
Case 6	with film	internal cooling, conjugate, lab condition	3D
Case 7	with film	adibatic, lab condition	3D

RESULTS AND DISSCUSSIONS

Evaluation of Heat Reduction Prediction Using Eq. 1 and Eq. 12: 2D Laboratory Condition

From the real system operating point of view, it is always desired to find out how much heat flux or wall temperature will actually be reduced after film is added into a system. As explained earlier, Eq. 1 has been widely used to evaluate the heat flux reduction because it is more difficult to measure heat flux than temperature. Examining the derivation process of Eq. 1 reveals that an implicit assumption of $T_{w,o}=T_{w,f}$ has been introduced implying that the wall surface temperature of the system without-film is assumed to be the same as that would occur with film-cooled condition.

To verify the validity of HFR calculation using Eq. 1, investigation starts with the 2D simulations of Case 1, 2 and 3. Heat flux directly obtained from CFD simulations of Cases 1 and 2 are shown as $(q"/q"_o)_{CFD}$ in Fig. 7. Note that there is no mathematical manipulation involved in this HFR value obtained from the CFD simulations. Calculations using Eq. 1 are then performed with three φ-values, 0.4, 0.6, and 0.9, respectively. Each φ-value is assigned as a single constant value for the entire surface; this is equivalent to assigning a constant surface temperature uniformly distributed over the entire surface irrespective of what the actual surface temperature distribution is. To evaluate the error introduced by applying a single φ-value, calculation of HFR using varying local wall temperature obtained from Case 2 is shown as $(q"/q"_o)_{vari}$. Observations of Fig. 7 are discussed below.

The CFD predicted heat flux ratio $(q"/q"_o)_{CFD}$ monotonously increases from a negative value (-0.2) immediately downstream of the film hole to 0.56 at the end of the computational domain, meaning the film performance downgrades downstream away from the film hole. A negative value of HFR means reversed heat transfer from the wall to the main flow. This is possible due to the heat conduction from the downstream hotter region into the near film hole cooler region, resulting in a higher wall surface temperature than the near-wall gas temperature. Thus, heat is transferred back into the film flow in the limited local area close to the film hole within the region x/d <6.

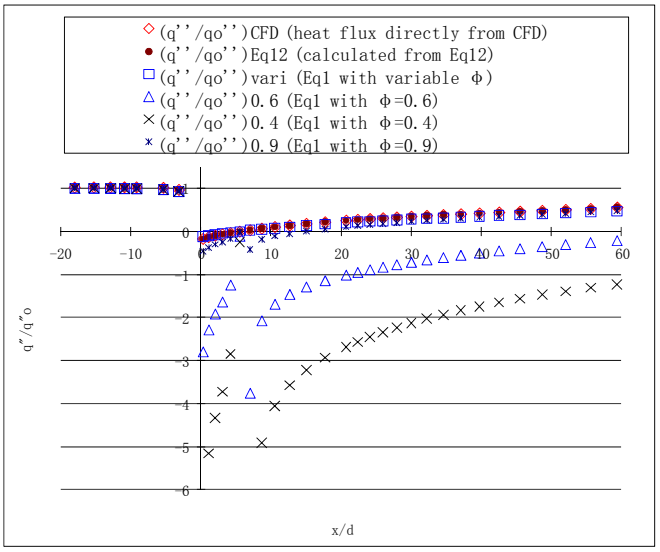

(a)

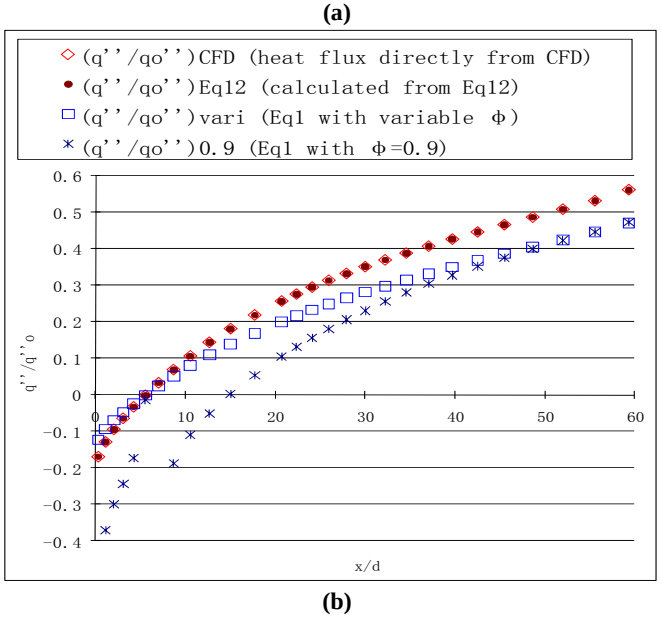

(b)

Figure 7 (a) Heat flux ratio (HFR) comparison between CFD predicted results and calculated results via Eq. 1. (b) An enlarged view of HFR (q"/q"$_o$) distributions to show four closely agreed cases and the region of heat flux reversal

The calculated HFR using Eq. 1 is very different from the CFD predicted conjugate case (Case 2) for using either φ=0.4 or 0.6 case. Negative values of HFR are found in most of the streamwise locations. As shown in Eqs. 1 and 3, a negative HFR is caused by $T_{aw}<T_w$, so the heat flow is reversed by moving from the wall to the mean flow. Usually, reversed heat flux is only possible in the limited region near the film hole where heat conduction from downstream in the metal wall is significant such as within x/d < 6 in Fig. 7. But in these two cases (φ =0.4 and 0.6), the negative heat flux prevails in the entire surface. This implies that the wall temperature corresponding to φ =0.4 or 0.6 (T_w = 360K and 340K, respectively) are higher than T_{aw} or, in other words, η is higher than φ, as can be seen in Fig. 8a & b. Consequently q" or HFR becomes negative from Eq. 3 or Eq. 1, respectively. This also implies that selection of φ =0.4 or 0.6 is artificial and does not adequately represent the physics of the currently simulated cases, which are under typical laboratory conditions. Note, in this study cases of φ = 0.4 and 0.6 correspond to T_w = 360K and 340K, respectively. Their values can be easily represented by horizontal lines and compared with T_{aw} and η in Fig. 8a &b.

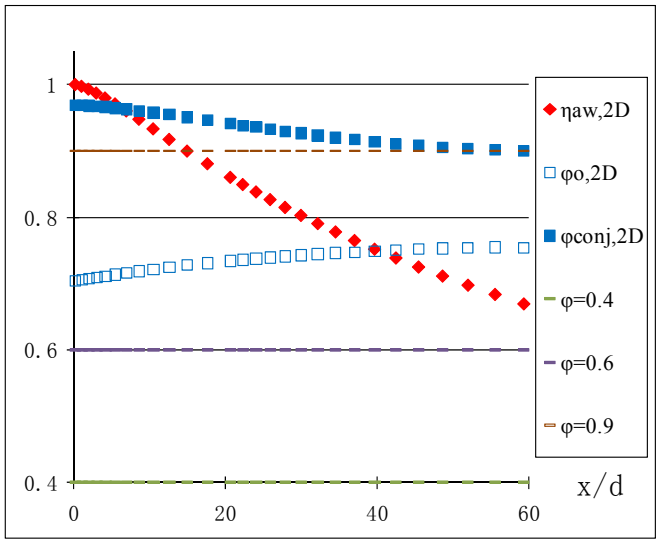

(a)

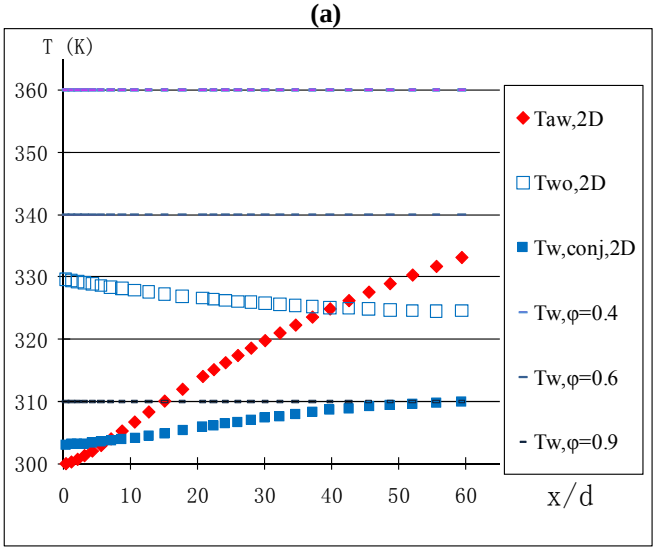

(b)

Figure 8 (a) Film cooling effectiveness (φ) and adiabatic film cooling effectiveness (η) (b) wall temperature.

Furthermore, these data have revealed another big issue: it is unrealistic to have any heat reduction more than 100%. For any part of the data where the HFR value dipped below 0 implies that film cooling actually feeds heat into the main flow with the thermal energy generated not from the main hot gas but from an artificially added source or sink! (HFR larger than 1 means film is not protecting the surface but rather it increases the surface heat transfer.) But what is the origin of this added artificial source or sink? It is from the imposed constant φ-value which corresponds to a constant T_w condition and serves as either an energy source or a sink depending on whether T_w is hotter or cooler than T_{aw}.

Among the three constant φ cases, φ=0.9 yields the closest results to the baseline case, but it over-predicts the heat flux reduction by more than 25% and the performance is not as good as the case using variable φ values.

Since using a single φ-value is not appropriate, it will be interesting to see how the calculated HFR results fare in Fig. 7 if the correct local φ-values obtained from CFD (Fig. 8a) are substituted into in Eq. 1. The results in Fig. 7 show the case using varying φ-values achieves a much better agreement to the conjugate baseline case predicted by CFD (Case 2). However, it is noticed that in the further downstream region, varying wall temperature calculation over-predicts heat reduction (i.e. a lower HFR value) by as much as 20% of the CFD predicted HFR. It is not clear why there is a 20% deviation because Eq. 1 is supposed to be theoretically exact and the deviation should be within the precision (not accuracy) of the CFD results. This 20% deviation prompts a re-examination of the accuracy of Eq. 1 as detailed below.

From the original derivation of HFR, it is implicitly implied that the wall temperature without film is the same as with the film, i.e. T_w in Eq. 3 is the same as in Eq. 4. However, in a real operation, adding coolant film will result in a change of airfoil temperature. The original derivation in Mick and Mayle's paper [1] was ambiguous in this issue and planted the seeds for confusion and errors when Eq. 1 was used later on. If the wall temperature change is taken into account between film-cooled (T_w, φ) and without film cases ($T_{w,o}$, φ_o), Eq. 1 can be re-derived and a revised equation is developed as follows.

$$\frac{q''}{q''_o} = \frac{h_{af}}{h_o}\frac{T_{aw}-T_w}{T_g-T_{wo}} = \frac{h_{af}}{h_o}\left(1-\frac{T_g-T_{aw}}{T_g-T_{wo}}+\frac{T_{wo}-T_w}{T_g-T_{wo}}\right)$$

$$= \frac{h_{af}}{h_o}\left(1-\frac{(T_g-T_{aw})/(T_g-T_j)}{(T_g-T_{wo})/(T_g-T_j)}\right)+\frac{h_{af}}{h_o}\frac{(T_{wo}-T_w)/(T_g-T_j)}{(T_g-T_{wo})/(T_g-T_j)}$$

$$= \frac{h_{af}}{h_o}\left(1-\frac{\eta}{\varphi_o}\right)+\frac{h_{af}}{h_o}\frac{(T_{wo}-T_w)/(T_g-T_j)}{\varphi_o}$$

$$= \frac{h_{af}}{h_o}\left(1-\frac{\eta}{\varphi_o}\right)+\frac{h_{af}}{h_o}\frac{(T_g-T_w)/(T_g-T_j)-(T_g-T_{wo})/(T_g-T_j)}{\varphi_o}$$

$$= \frac{h_{af}}{h_o}\left(1-\frac{\eta}{\varphi_o}\right)+\frac{h_{af}}{h_o}\frac{\varphi-\varphi_o}{\varphi_o} \qquad (12)$$

Where $\varphi_o = (T_g-T_{w,o}) / (T_g-T_j)$ (13)

The difference between Eqs. 1 and 12 is:

$$\left(\frac{q''}{q''_o}\right)_{eq12}-\left(\frac{q''}{q''_o}\right)_{eq1} = \frac{h_{af}}{h_o}\left(1-\frac{\eta}{\varphi_o}\right)+\frac{h_{af}}{h_o}\frac{\varphi-\varphi_o}{\varphi_o}-\frac{h_{af}}{h_o}\left(1-\frac{\eta}{\varphi}\right)$$

$$= \frac{h_{af}}{h_o}\left(\frac{\eta}{\varphi}-\frac{\eta}{\varphi_o}+\frac{\varphi-\varphi_o}{\varphi_o}\right) = \frac{h_{af}}{h_o}\left(\frac{\eta\varphi_o-\eta\varphi+\varphi^2-\varphi\varphi_o}{\varphi\cdot\varphi_o}\right)$$

$$= \frac{h_{af}}{h_o}\frac{(\varphi-\eta)\cdot(\varphi-\varphi_o)}{\varphi\cdot\varphi_o}$$

Since the wall temperature of a system without film will supposedly be lowered after the film is added (which is the purpose of film cooling), φ should be larger than φ_o. And typically, $T_w < T_{aw}$ because heat is transferred from the heat source (main flow) into the wall. As a result, φ is generally higher than η. Thus $\frac{(\varphi-\eta)\cdot(\varphi-\varphi_o)}{\varphi\cdot\varphi_o} > 0$ and as a result, Eq. 1 under-predicts HFR and over-predicts the actual heat flux reduction.

It must be noted here that exceptions for both conditions ($T_w < T_{wo}$ and $T_w < T_{aw}$) are possible when the conjugate wall conduction and the flow's 3D effects are not negligible. Examples as studied in the following 3D simulations demonstrate those exceptions clearly. But those exceptions should only happen in a limited region and should not prevail in the whole blade area; otherwise, the fundamental goal of using the film to protect the airfoil surface is overturned and the fact that the only heat source being the main flow is violated. The practice of using heated surface to simulate film cooling heat transfer scenario contribute to those exceptions and are subjected to detailed discussion in [12].

Mick and Mayle's equation (Eq. 1) yields reasonable estimate for HFR in studies where adding film does not change the wall temperature greatly, in which case $\varphi \approx \varphi_o$, $\frac{(\varphi-\eta)\cdot(\varphi-\varphi_o)}{\varphi\cdot\varphi_o} = 0$, so Eq.12 gives the same results as Eq. 1. But when the change in φ after adding the film is not negligible, all factors of φ, φ_o and η must be considered to give the accurate HFR through Eq. 12.

Comparisons of HFR directly from simulations and calculation results from Eq. 1 and Eq. 12 are also shown in Fig. 7. An excellent agreement is found between the CFD simulation and the calculated results based on Eq. 12, as it is supposed to be since Eq. 12 is theoretically exact within the CFD precision.

Strong irregularities of HFR curves of all three cases using a single φ-value for each case are noticed around x/d=5.6. These irregularities are caused by the divergence of h_{af} in the conjugate case (Case 2) when T_w approaches T_{aw} and heat flux is approaching zero and undergoing reversal of direction. This is very different from the continuous smooth curves in the case of the CFD predicted HFR and the varying wall temperature case calculated via Eqs. 1 or 12; both cases bear the correct physics.

Simulation at Elevated Gas Turbine Operating Condition

To verify the statement that the conclusion arrived in the previous discussions based on lab conditions should not be significantly affected by the elevated operating conditions in a gas turbine system, cases under elevated condition are simulated in Cases 4.1, 4.2 and 4.3 in the same manner as in Cases 1, 2 and 3, only with different boundary conditions.

The results of HFR are plotted in Fig. 9, corresponding to Fig. 7 under the lab condition. Only minor differences can be found when compared with the HFR results from the lab condition simulation. The magnitude of the reversed heat flux is reduced near the injection hole. All the issues discussed and conclusions made in the previous section with the laboratory conditions are valid under elevated gas turbine operating condition.

3D Simulation Study

Based on the physics discussed in the 2D cases, complexity of 3D flow filed is introduced and analyzed in the 3D simulations.

Figure 10 shows the 3D disposition of iso-thermal surfaces of Case 5. The iso-surfaces can be regarded as discrete layers of films at different temperatures overriding the airfoil. The inner

layer of film, at 380K as shown in this study, is cooler but covers a smaller portion of the foil. The concept of injecting a coolant to form film layers over the airfoil to protect the surface from the hot main flow is well demonstrated in this figure.

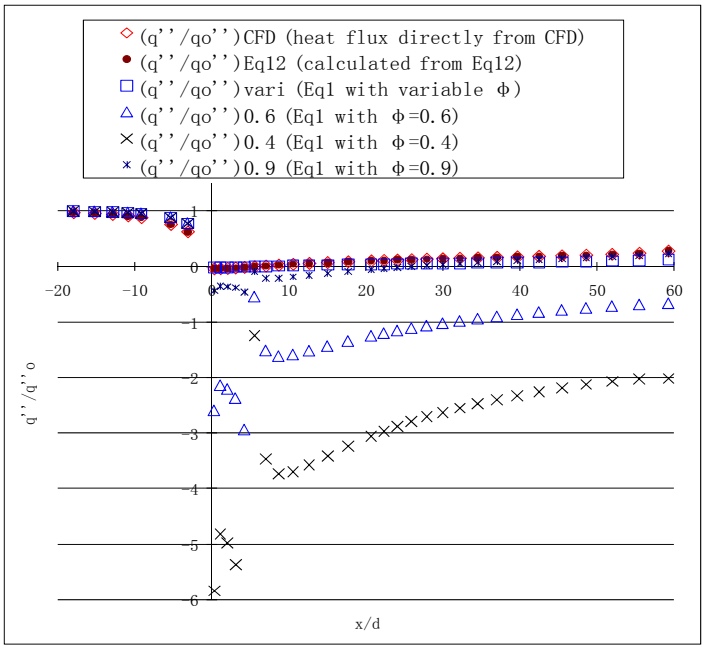

(a)

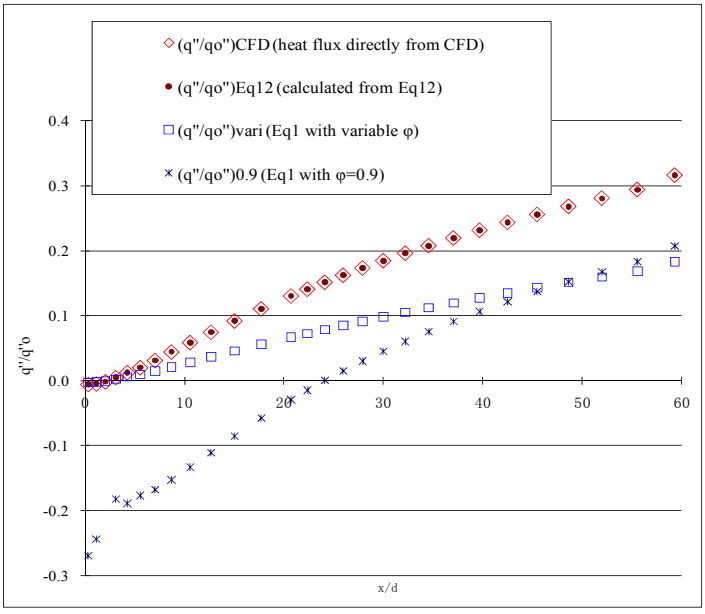

(b)

Figure 9 2D elevated GT condition (a) Heat flux ratio (HFR) comparison between CFD predicted results and calculated results via Eq. 1. (b) An enlarged view of HFR (q"/q"$_o$) distributions to show four closely agreed cases and the region of heat flux direction reversal

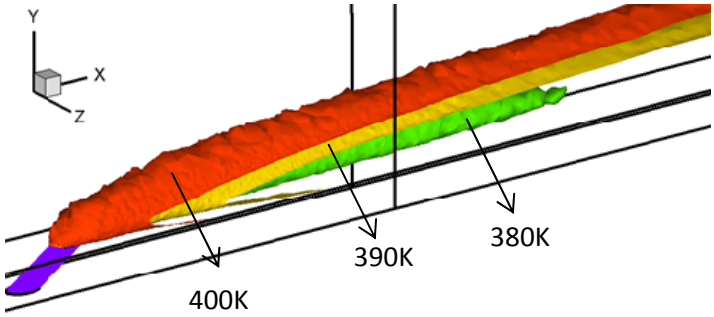

Figure 10 Iso-thermal surface in adiabatic wall case

Film cooling effectiveness and wall temperature from the 3D cases of Case 5, 6 and 7 are plotted in Fig. 11 (a) and (b), respectively. Temperatures from the corresponding 2D cases are also plotted in the same figure for comparison. Temperature contours of 2D and 3D adiabatic wall cases on the mid-plane are shown in Fig. 12. Figure 13 shows the wall surface temperature contours for Case 6 (3D conjugate wall with internal cooling) and Case 7 (3D, adiabatic wall). And heat flux contour of Case 6 is shown in Fig. 14.

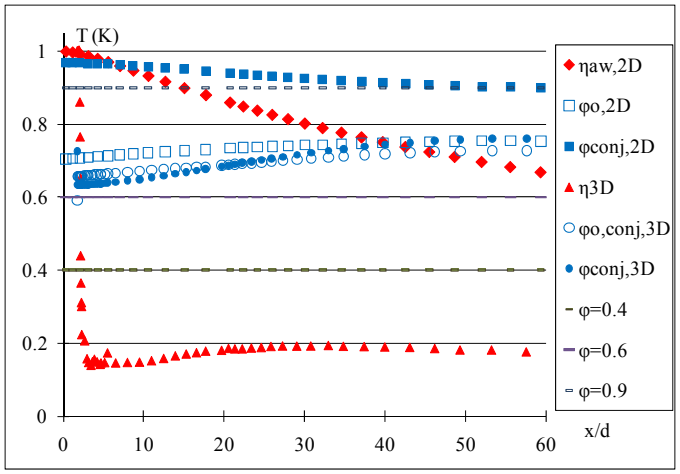

(a)

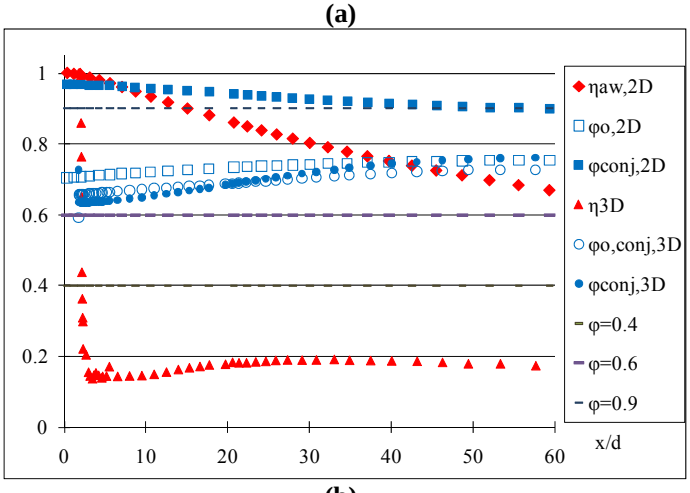

(b)

Figure 11 3D cases (a) Film cooling effectiveness (φ) and Adiabatic film cooling effectiveness (η) (b) wall temperature.

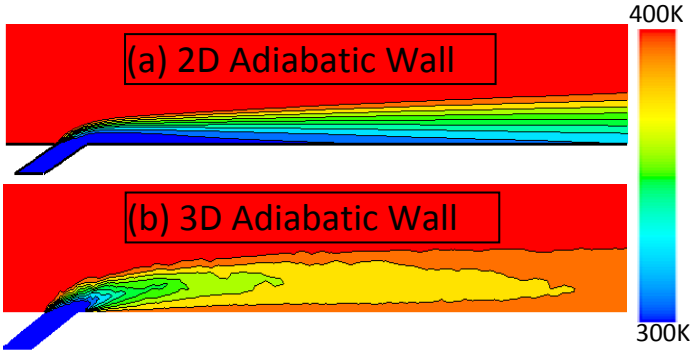

Figure 12 Temperature contours of (a) Case 3 (2D) and (b) on the midplane of Case 7 (3D)

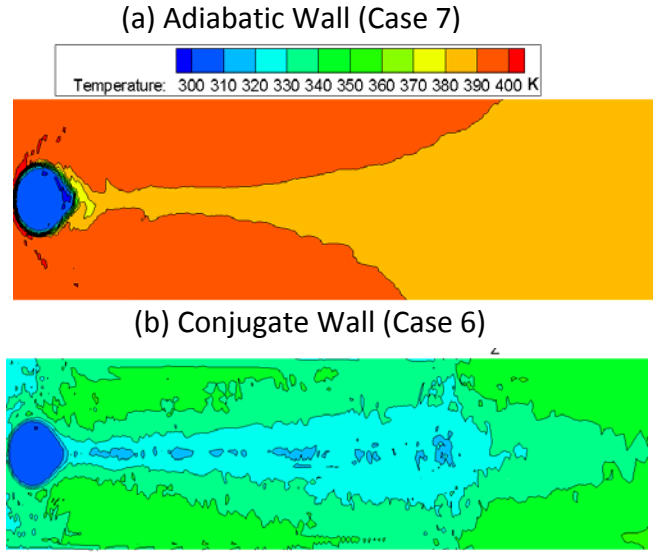

Figure 13 Test surface temperature contours of (a) Case 7 and (b) Case 6

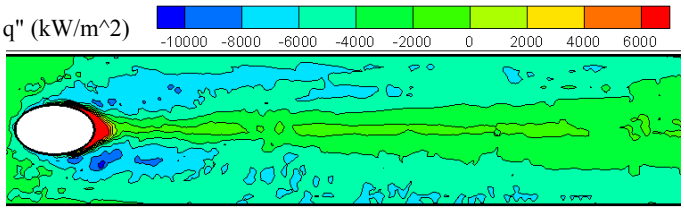

Figure 14 Test surface heat flux contours of 3D conjugate Case (Case 6)

Comparing the adiabatic film effectiveness in 3D cases with the 2D cases, it is found that 3D cases produce much lower η than 2D cases. Also it is noticed that η in 3D cases is more uniform in most part of the blade as opposed to 2D cases in which η decays from about 1.0 to 0.65. This is due to the enhanced 3D flow mixing and roll-up characteristics in 3D cases as can be seen in Fig. 12. In 2D cases, the film does not have an "escape" mechanism, so that coolant flow has to layer on top of the blade surface to generate an ideal protecting film. Heat from the hot main flow must penetrate the film first and then passes onto the blade surface, which is the ideal scenario for film cooling schemes. On the other hand, in 3D cases the mixing between the film and the main flow is stronger with the addition of mixing in lateral direction (Z direction as shown in Fig. 10), resulting in the film being heated up more quickly thus less effective in reducing surface temperature than in 2D cases. Moreover, since coolant film only covers part of the blade around the centerline as shown in Fig. 13, the hot main flow penetrates in between film coverage, touches the blade or wraps around from the lateral direction to reach the bottom of the film. All those factors, such as the stronger mixing and lateral roll-up flow structure, contribute to a more uniform but less effective film cooling in 3D cases than in 2D cases. More detailed discussion of the secondary flow structure in film cooling flow is referred to Wang and Li [13], Haven and Kurosaka [14].

It is also noticed in Fig. 11 that for the 3D cases the wall temperature of the conjugate case without film (Case 5) does not change much after the coolant is injected (Case 6). This seemingly suggests that film cooling does not cool down much of the surface temperature because internal cooling is already effective. However, from the heat flux reduction results for 3D cases in Fig. 15, it is found that the net heat flux reduction (NHFR =1-HFR) can reach as high as 80% near the injection hole and decays to about 20% further downstream. This large heat flux reduction does not seem to be suggested by the slightly changed wall temperature (with a value less than 2% of T_g-T_j) or φ value. The reason for the relatively minor reduction in wall temperature is that heat conduction within the metal blade smears the temperature variance making the blade temperature more uniform. Moreover from Fig.11, it is found that T_{aw} of the 3D case is significantly higher than T_{wo}, suggesting that the internal cooling is more effective than film cooling in the studied conditions. T_{wo} of the no-film case is subject to internal cooling only, thus T_{wo} shows the effectiveness of the internal cooling, while T_{aw} shows the film cooling effectiveness.

This case serves as a good example to demonstrate that in the conditions where internal cooling and conjugate wall effect are significant, the value of the overall cooling effectiveness (φ) alone is not sufficient in determining the film cooling performance as in the adiabatic cases. The additional information from HFR results is essential to evaluate the overall film cooling performance under those conditions.

One surprising finding in Fig. 11 is that when the 3D case without film (Case 5) is compared with the film-cooled case (Case 6), the wall temperature of Case 5 is slightly lower than Case 6 in the near injection hole area. This is against intuition since the wall temperature is expected to be reduced after cooling film is injected, and no similar situation is found in 2D cases either. Explanation of this phenomenon can be obtained through the investigation into the flow field. As it can be seen in the cross-sectional flow field in Fig. 16, a strong jet flow (coming out of the paper) through the injection hole induces flow wrapping from the side towards centerline. The lateral flow entrainment in the 3D case brings in the hot gases from the main flow, thus larger heat flux from the main flow is transferred into the airfoil in Case 6, resulting in a slightly higher wall temperature than without the film. But as coolant film diffuses along the flow direction, the cooling film fulfils its function, and as a result the blade is cooler with a higher $\varphi_{conj,3D}$ than $\varphi_{o,conj,3D}$ as shown in Fig. 11.

Examining the HFR results from Fig. 15, again it is found that the revised HFR equation (Eq. 12) matches the CFD results best. Calculations using Eq. 1 with constant φ values give better estimated results than in 2D case because the streamwise surface temperature is more uniform in the 3D cases, but they are still off from the correct value. Using φ=0.4 results in as much as 25% difference from the CFD results.

Similar to 2D studies, the reversed heat flux region is also found. But the region is smaller than in 2D cases due to the stronger 3D flow mixing effect.

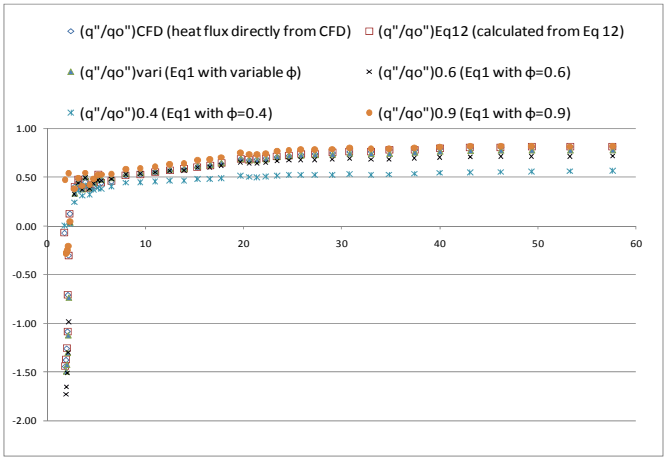

(a)

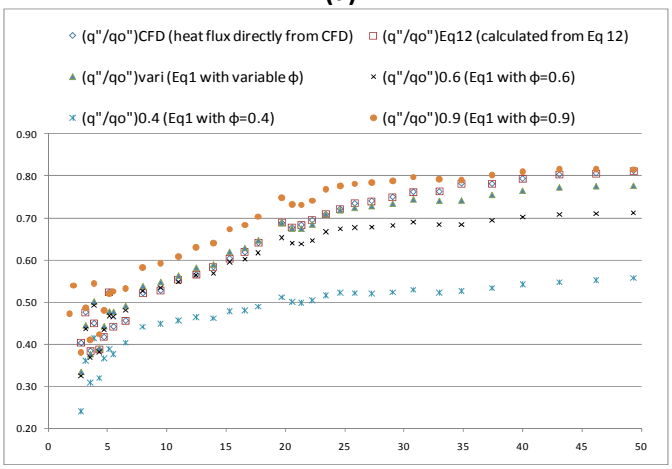

(b)

Figure 15 3D study (a) Heat flux ratio (HFR) comparison between CFD predicted results and calculated results via Eq. 1 and 12 (b) An enlarged view of HFR (q"/q"$_o$) distributions (Use a different symble for the φ=0.4 case)

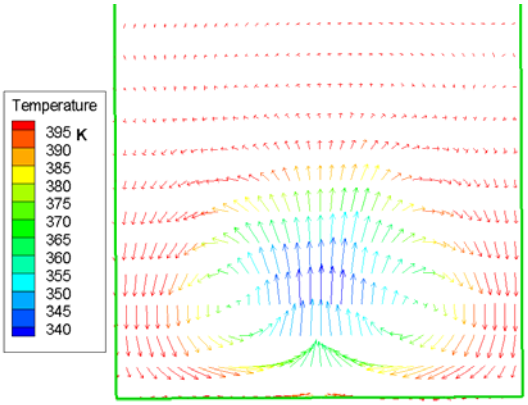

Figure 16 Cross-sectional velocity vector plot at x/d=1 for Case7

CONCLUSION

In this study, the Heat Flux Ratio (HFR) equation originally derived by Mick and Mayle [1] is closely investigated and the derivation process of the equation is re-examined in details. Some concerned issues raised by employing constant values of φ to calculate HFR are identified and extensively discussed. Examining the original derivation process of Eq. 1 reveals that an implicit assumption of $T_{w,o}=T_{w,f}$ has been introduced implying that the wall surface temperature of the system without-film is assumed to be the same as that would occur with film-cooled condition. A revised equation is derived and wall temperature change is taken into account between the film-cooled (T_w, φ) and without film cases ($T_{w,o}$, φ_o). A series of computational experiments are designed and conducted to study the concerned issues of Eq. 1 and verify the validity of the newly derived Eq. 12 under different conditions.

The new HFR equation is summarized as follows.

$$\frac{q''}{q''_o}=\frac{h_{af}}{h_o}\left(1-\frac{\eta}{\varphi_o}\right)+\frac{h_{af}}{h_o}\frac{\varphi-\varphi_o}{\varphi_o} \quad \text{(Heat Flux Ratio, HFR)} \qquad (12)$$

$\eta = (T_g-T_{aw}) / (T_g-T_j)$ (Adiabatic film cooling effectiveness) (2)

$h_{af} = q'' / (T_{aw}-T_w)$ (Adiabatic heat transfer coefficient) (3)

$h_o = q''_o / (T_g-T_w)$ (Heat transfer coeff. without film cooling) (4)

$\varphi = (T_g-T_w) / (T_g-T_j)$ (Film cooling effectiveness) (5)

$\varphi_o = (T_g-T_{w,o}) / (T_g-T_j)$ (Cooling effectiveness without film) (13)

Results reveal that the origin of the unrealistic negative HFR given by the constant φ cases arise from the assumption of a wall temperature that the system can't possibly achieve. Using the values for φ (0.5 ~ 0.7) as a single constant to calculate the heat flux ratio (HFR) is questionable. Implicitly, a constant φ-value implies a constant film cooling effectiveness or a constant T_w over the entire surface, which is usually not the case in real conditions. Negative values of film cooling effectiveness (φ) occurs in some simulated cases showing the commonly adopted value φ=0.5~0.7 induces errors and could give a false HFR. The φ-value must be actually related to the h-value from the same experiment and is obtained under the same condition (T_g, T_f, Re, M) except one is internally cooled and the other one has an adiabatic wall. It is not correct to use the η value from an experiment or CFD analysis, while use the φ value from other sources as the "given φ value" or as an

independent free parameter that can be just plugged into Eq.12 to calculate HFR.

Employing variable φ in the original equation (Eq.1) gives more reasonable results but still generates over-predicted heat reduction (lower HFR) by as much as 20% of the simulated prediction in some cases.

An excellent agreement is found between the CFD simulation and the calculated results based on the newly developed Eq. 12. The difference between the old and new equations can contribute to about 20% of the heat flux ratio value.

A conjugate wall cooling simulation shows that reversed heat transfer from surface to gas that gives a negative HFR is possible due to the heat conduction in the metal base from the downstream hotter region into the near film hole cooler region. But it is only limited to near film hole region and should not prevail in the entire airfoil.

The conclusions drawn from the laboratory conditions are supported by the CFD results obtained under elevated gas turbine operating conditions, although the magnitude of reversed heat flux is reduced near the injection hole.

3D cases produce lower but more uniform η's than 2D cases due to the stronger 3D flow mixing effect, making film cooling less effective. Conjugate wall makes a significant effect on 3D cases by smearing the temperature variation and making the blade temperature more uniform. It is also demonstrated that under conditions where internal cooling and the conjugate wall effect are significant, a small change of wall temperature (or φ) can achieve appreciable heat flux reduction. The 3D result also shows that a slightly increased wall temperature may occur near the injection hole when film cooling is applied due to film-induced 3D flow mixing. The heat flux values calculated using the newly derived HFR equation always produces correct heat flux values and directions (positive or negative) for all conditions including reversed heat flow, conjugate wall, and 3-D mixing.

ACKNOWLEDGEMENT

This study is supported by the Louisiana Governor's Energy Initiative via the Clean Power and Energy Research Consortium (CPERC) and administered by the Louisiana Board of Regents.

REFERENCE

[1] W.J. Mick, R.E. Mayle, Stagnation film cooling and heat transfer, including its effect within the hole pattern, ASME J. of Turbomachinery 110 (1988) 66-72.

[2] The Gas Turbine Handbook, Office of Fossil Energy, National Energy Technology Labatory, U.S. Department of Energy, 2006, PP. 310-318.

[3] B. Sen, D.L. Schmidt, and D.G. Bogard, Film cooling with compound angle holes: heat transfer, ASME J. of Turbomachinery 118 (1996) 800-806.

[4] S. Ou, J.C. Han, Influence of mainstream turbulence on leading edge film cooling heat transfer through two rows of inclined film slots, ASME International Gas Turbine and Aeroengine Congress and Exposition 36, 1991.

[5] Y. Lu, A. Dhungel, S.V. Ekkad, R.S. Bunker, Effect of trench width and depth on film cooling from cylindrical holes embedded in trenches, ASME J. Turbomachinery 131 (1) (2009) 011003.

[6] C.M. Bell, H. Hamakawa1, P.M. Ligrani, Film cooling from shaped holes, ASME J. Heat Transfer, 122 (2000) 224-232.

[7] R.A. Brittingham, J.H. Leylek, A detailed analysis of film cooling physics: Part IV—compound-angle injection with shaped holes, ASME J. Turbomachinery 122 (2002) 133-145.

[8] Fluent Manual, Version 6.2.16, Fluent, Inc. 2005.

[9] X. Li and T. Wang, Effects of various modeling on mist film cooling, ASME Journal of Heat Transfer 129 (2007) 472-482.

[10] R. J. Goldstein, P. Jin, and R. L. Olson, Film Cooling Effectiveness and Mass/Heat Transfer Coefficient Downstream of One Row of Discrete Holes, J. Turbo mach. 121 (1999), 225-232

[11] L. Zhao and T. Wang, An Investigation of Adiabatic Wall Temperature as the Driving Temperature in Film Cooling Studies, GT2011-46012, manuscript submitted to ASME Turbo Expo2011, Vancouver, Canada, June 6-10, 2011

[12] L. Zhao and T. Wang, Discussion on the Practice of Using Heated Surface in Film Cooling Studies, GT2011-46614, manuscript submitted to ASME Turbo Expo2011, Vancouver, Canada, June 6-10, 2011

[13] T. Wang, X. Li, Mist film cooling simulation at gas turbine operating condition, International Journal of Heat and Mass Transfer, 51 (2008) 5305–5317.

[14] B.A. Haven, M. Kurosaka, Kidney and anti-kidney vortices in crossflow jets, Journal of Fluid Mechanics, 352 (1997) 27-64.